Study of the Origin and Mechanism of Band Broadening and Pressure Drop in Centrifugal Partition Chromatography

ARTICLE *in* ANALYTICAL CHEMISTRY · DECEMBER 1988

Impact Factor: 5.64 · DOI: 10.1021/ac00173a017 · Source: PubMed

3 AUTHORS, INCLUDING:

Daniel W. Armstrong
University of Texas at Arlington
678 PUBLICATIONS **24,430** CITATIONS

SEE PROFILE

Alain Berthod
Claude Bernard University Lyon 1
260 PUBLICATIONS **5,857** CITATIONS

SEE PROFILE

Study of the Origin and Mechanism of Band Broadening and Pressure Drop in Centrifugal Countercurrent Chromatography

Daniel W. Armstrong,* Gary L. Bertrand, and Alain Berthod[1]

Department of Chemistry, University of Missouri—Rolla, Rolla, Missouri 65401

The theory of nonequilibrium band broadening and factors giving rise to back pressure in countercurrent chromatography (CCC) and centrifugal CCC have not been considered adequately. Plots of efficiency versus flow rate show behavior roughly opposite that of modern liquid chromatography (LC) or gas chromatography (GC). Indeed, van Deemter-type plots have maxima rather than minima. Consequently, the best efficiency is obtained at very high or very low flow rates. A model to explain this behavior is formulated and discussed. Equations based on this model are derived and evaluated by using experimental results. The pressure drop in centrifugal CCC arises from both hydrostatic and hydrodynamic factors. An equation is derived that relates all relevant physicochemical factors to the system pressure drop. When the optimum experimental and instrumental parameters are chosen, the effect on selectivity, efficiency, and pressure drop must be considered carefully.

Countercurrent chromatography (CCC) is a liquid–liquid chromatographic method in which the liquid stationary phase is held in the bed by a gravitational or centrifugal field rather than by an inert solid support. Ito first introduced CCC as a method that could obtain separations analogous to stepwise liquid–liquid extraction but in a continuous chromatographic mode (*1*). Since its introduction, Ito and others have made a variety of different CCC instruments. Several designs are based on a helical coil that is placed in an acceleration field (*2–4*). Another approach is taken in locular CCC where a series of straight tubes are partitioned into several cylindrical chambers (*5–7*). Each partition has a small hole in the center that allows the flow of mobile phase from chamber to chamber. Placing these tubes at some angle to the horizon (generally 20–45°) allows one to immobilize a relatively constant volume of stationary liquid (*7*). In droplet CCC several vertical columns are connected in series by capillary tubes. The system is filled with stationary phase and the mobile phase is pumped through it as a stream of droplets (*8, 9*). Centrifugal CCC is sometimes referred to as centrifugal partition chromatography (CPC) and is a technique that is closely related to droplet CCC. The main difference is that horizontal channels machined into inert plates are used instead of vertical glass columns and that centrifugal force is used to phase separate the solvents rather than gravity as in droplet CCC (see Figure 1). The net result is a more efficient and flexible system (*10*). For example, a CPC unit can have roughly an order of magnitude more plates than other CCC devices but still carry out identical separations in less time (*10, 11*).

The advantages of CCC or CPC over traditional LC for preparative and other separations are well documented (*1–10*). They have been successfully utilized for a range of applications, including the separation and purification of synthetic organics, natural products, and whole particles and cells (*12*).

[1] On leave from Laboratoire des Sciences Analytiques, Universite de Lyon-1, U.A. CNRS 435, 69622 Villeurbanne, France.

Theoretical and mechanistic treatments of CCC or CPC are not extensive (*13, 14*). In general, separations are assumed to occur via classical partitioning as in liquid–liquid extraction. Thus far, there have been no nonequilibrium treatments analogous to those developed by van Deemter (*15*), Giddings (*16*), and Golay (*17*) for other modes of chromatography. In addition, there has been no consideration of the factors controlling the pressure drop in CCC or CPC and how it affects the separation experiment (back pressure is generally a more significant problem in CCC methods that use centrifugal fields). In this work we demonstrate that CCC or CPC is a relatively linear but kinetically controlled technique, as in many other forms of chromatography. However, a van Deemter-type plot for centrifugal CCC is very different from those of traditional GC or LC. A model and expression that explains the observed band broadening and the shape of the flow rate–efficiency curve is formulated. In addition, an equation that relates relevant parameters to pressure drop is derived.

EXPERIMENTAL SECTION

Materials. The CPC experiments were performed with a centrifugal countercurrent chromatograph, Model CPC-NMF, from Sanki Laboratories, Inc., Sharon Hill, PA. This apparatus consists of up to 12 cartridges placed in the rotor of a centrifuge. Each cartridge is composed of four poly(chlorotrifluoroethylene) (PCTFE) plates alternately sandwiched between five Teflon sheets. Each PCTFE plate bears 100 channels engraved in two rows of 25 on each side.

Figure 1 shows the channel design. For clarity, only portions of 6 channels, instead of 50, have been drawn. In each row, the top of the channel is connected to the bottom of the next one. The top of the last channel of a row is connected to the bottom of the first channel of the next row, either through a duct on the same side of a PCTFE plate or through a hole across the plate to the other side. The liquid must travel through the 100 channels of a PCTFE plate, then it goes to the next plate, through the 400 channels of a cartridge. Up to twelve cartridges can be connected in series. During operation at 800 rpm the internal volume of a cartridge is approximately 20 mL, corresponding to about 50 μL per channel and connecting duct. When the centrifuge rotor is loaded with six cartridges, the internal volume from the injection valve to the detector output is 125 mL.

The rotor is enclosed in a constant temperature box; all experiments were done at 25 °C. A classical LC chromatograph pump (Shimadzu, Model LC 6A or Waters, Model 590) was used. The Sanki command module (Model CPC-FCU-V) allowed one to inject a sample and to choose between the ascending or descending mode. The detector was a Shimadzu, Model SPD-6A, UV–vis detector equipped with a preparative flow cell. The recorder was from Linear, Inc., Model 1200.

All solvents were HPLC grade and obtained from Fisher. Hydroquinone, pentachlorophenol, (2,2,2-trichloroethylidene)-bis(chlorobenzene) (DDT), (2,2-dichloroethylidene)bis(chlorobenzene) (DDD), and 1-naphthol were obtained from Aldrich and used as received.

Methods. Two very different liquid systems were used. The first system was methanol–hexane. Those two liquids have low densities (0.791 and 0.661 g/cm^3 at 20 °C, respectively), low viscosities (0.54 and 0.29 cP at 25 °C, respectively) and a mutual solubility sufficiently high that is was necessary to add 1% (v/v) of water in methanol to decrease the hexane solubility. The added

0003-2700/88/0360-2513$01.50/0

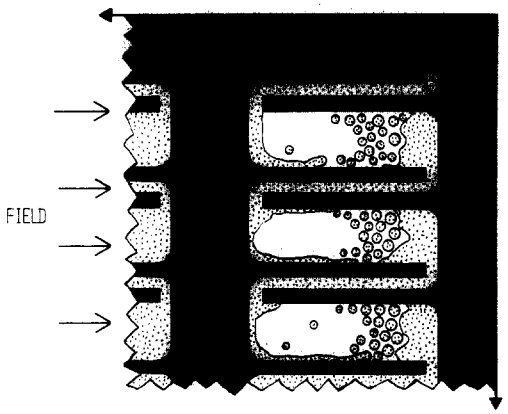

Figure 1. Schematic showing the shape and arrangement of channels engraved into the PCTFE plates of a centrifugal CCC device. In actuality there are two parallel rows of 25 connected channels on each side of the plate (100 total). Also shown is the direction of the field, the stationary and mobile phase solvents, the emulsified layer that forms at the phase boundary (which is flow rate dependent) and the direction of flow. Key: PCTFE plate, black area; stationary phase, white area; mobile phase, dotted pattern.

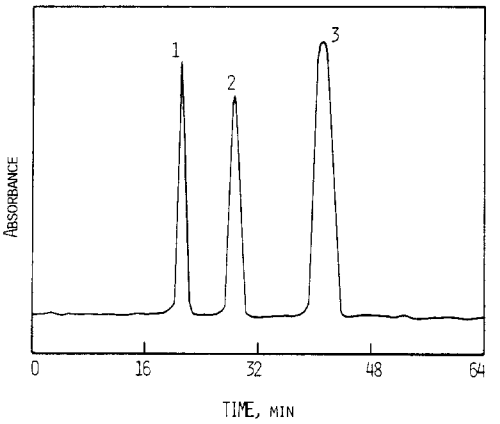

Figure 2. Centrifugal CCC chromatogram showing the separation of (1) 1-naphthol, (2) DDD, and (3) DDT. The stationary phase was hexane, the mobile phase was methanol + 1% water (by volume), the rotation rate was 1300 rpm, the flow rate was 3.0 mL/min, the wavelength of detection was 230 nm, and the separation was done in the descending mode.

water also served to increase the interfacial tension and density difference between the two liquid phases. The second liquid system was octanol–water. Octanol has a high viscosity (3.6 cP at 25 °C) and a relatively low density (0.845 g/cm^3 at 25 °C). The first system was chosen for its convenience to handle, the phase saturation process is fast, and the two phases have relatively similar polarities, which produces low values for the partition coefficients of a variety of solutes. The second system was chosen because it is the reference system for the study of the "hydrophobic bonding" of active drugs in biochemistry and pharmaceutical chemistry. The physicochemical properties of the equilibrated phases (one liquid saturated with the other) are quite different from those of the pure liquids.

The stationary phase is maintained in each channel by the centrifugal field created by the spinning rotor. The mobile phase passes through the stationary phase as small droplets or streams (at higher flow rates) moving in the centrifugal field (Figure 1). Streaming tends to occur along the walls of the chamber and can sometimes flow in a helical pattern when the chambers are rotating in the centrifuge. In the ascending mode, the stationary phase is the lower or outer, denser liquid and the mobile phase is the less dense liquid. The mobile phase moves from the bottom to the top of the cartridge though the stationary phase against the centrifugal field.

Efficiency data for the van Deemter plots was generated for three different solutes (DDT, DDD, and 1-naphthol) in the hexane–(methanol/water) system and for two solutes (hydroquinone and pentachlorophenol) in the octanol–water system. The flow rate was varied between 0.1 and 6.0 mL/min while maintaining all other conditions constant. The number of theoretical plates (n) for each separation was calculated by using the standard equation

$$n = 16\left(\frac{t_r}{W_b}\right)^2 \quad (1)$$

where t_r is the retention time and W_b is the peak width at the base line. A typical chromatogram obtained with the hexane–methanol and water system is shown in Figure 2.

RESULTS AND DISCUSSION

The effect of flow rate on efficiency was studied for five different compounds in two different liquid–liquid systems (see Experimental Section). In traditional van Deemter expressions for gas and liquid chromatography, the height equivalent to a theoretical plate (HETP or H) is plotted vs flow rate. There is no formal column in centrifugal CCC but rather a series of connected channels. In order to make a van Deemter-type plot for CPC, one must plot (2400/n), where 2400 is the number of channels used in each experiment and

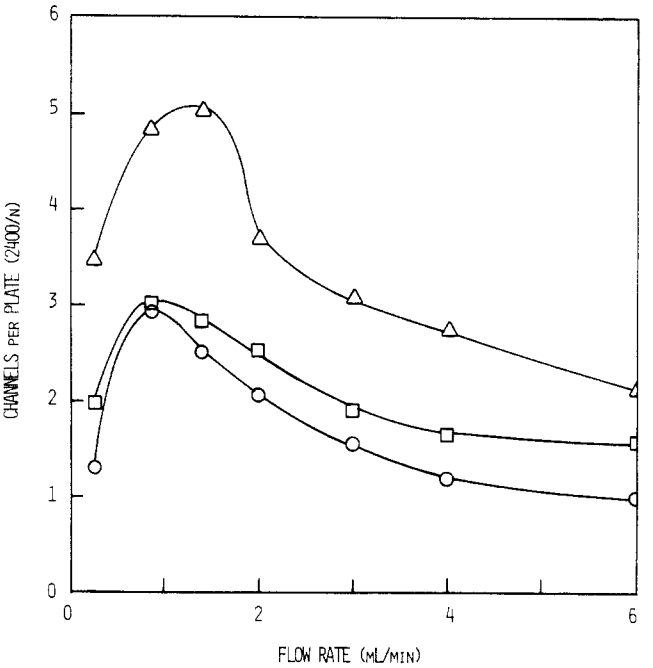

Figure 3. van Deemter-type plots of flow rate versus channels/plate for centrifugal CCC. In this experiment the stationary phase was hexane, the mobile phase was methanol + 1% water (v/v), the temperature was 20 °C, the rotor spin rate was 1100 rpm, and the amount of each solute injected was 80, 200, and 400 μg for β-naphthol, DDC, and DDT, respectively. Six cartridges containing 2400 channels were used.

n is the empirically determined plate number. The ratio 2400/n represents the number of channels needed to produce one theoretical plate. Figures 3 and 4 show the effect of flow rate on efficiency for several solutes in a hexane–methanol–/water system and octanol–water system, respectively. This data is graphed in the same way as most traditional van Deemter plots for gas and liquid chromatography. Several things are apparent from this data. First of all, the plots for centrifugal CCC are essentially opposite to those for GC and LC (i.e., there are maxima rather than minima). It appears that the optimum separation efficiency occurs at very low or very high flow rates. It also appears that the position and height of the maxima are affected by the viscosity of the mobile phase and the retention characteristics of the compound used in the study. In view of these results, the question arises as to whether or not traditional nonequilibrium treatments for chromatography are applicable to CCC tech-

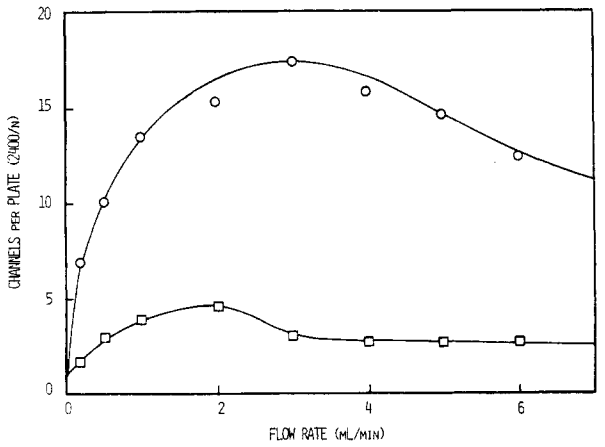

Figure 4. van Deemter-type plots for hydroquinone (□) and pentachlorophenol (○). Experimental conditions were identical with those in Figure 2 except that the stationary phase was water and the mobile phase was octanol. The viscosity of octanol is greater than that generally recommended for CCC.

niques. This question and possible answers to it are addressed in the following paragraphs.

Traditional Kinetic Formulations. The overall plate-height equation for liquid chromatography is

$$H = H_L + H_s + H_m + H_{sm} \quad (2)$$

where H is the total height equivalent to a theoretical plate, H_L is the plate height contribution for longitudinal diffusion, H_s is the stationary phase mass transfer, H_{sm} is the stagnant mobile phase contribution, and H_m is the moving mobile phase effect. H_m includes terms for eddy diffusion and diffusion due to concentration gradients, H_D. These are frequently combined as suggested by Giddings (*16*) to

$$H_m = \frac{1}{1/H_e + 1/H_D} \quad (3)$$

Several of these terms may not be applicable to centrifugal CCC. For example, H_L is not needed even at very low flow rates, as the unit cell limits this type of diffusional band broadening. As there is no porous stationary phase that traps "pools" of mobile phase, H_{sm} is superfluous. In CPC, the maximum efficiency limit appears to be 1 plate per channel. However in LC and GC the maximum obtainable efficiency is often controlled by the eddy diffusion term H_e, which is not applicable in CPC. It appears that H_s and H_m (where $H_m = H_D$) are the only terms from conventional theory that apply to CPC. By use of the van Deemter–Golay approach this expression would be

$$H = T_s\nu + T_m\nu \quad (4)$$

where ν is the mobile phase flow velocity, T_s is a collection of terms related to stationary phase mass transfer, and T_m is the analogous collection of terms for mobile phase mass transfer. Both T_s and T_m are known for packed (*15*, *16*) and open tubular (*17*, *18*) columns as shown below

$$H_{(packed)} = \frac{k'}{(1+k')^2}\frac{qd_f^2}{D_s}\bar{\nu} + \frac{\beta d_p^2}{D_m}\bar{\nu} \quad (5)$$

$$H_{(ot)} = \frac{k'}{(1+k')^2}\frac{\theta d_f^2}{D_s}\bar{\nu} + \frac{Kr^2}{D_m}\bar{\nu} \quad (6)$$

where k' is the capacity factor of a solute, d_f is the diffusional length related to the stationary phase thickness, D_s is the diffusion coefficient of a solute in the stationary phase, q is a "configuration factor", d_p is the diameter of the stationary phase packing, D_m is the diffusion coefficient of a solute in the mobile phase, and β is a system parameter that depends on the geometry of the packing, channels and so on. In the case of open tubular columns d_p is replaced with the radius of the column, r, and the system constants q and β are replaced with constants θ and K, which better take into account the properties and behavior of capillary tubes. There have been numerous discussions of the factors that comprise these constants (*16*, *18–20*).

Although analogies can be made between centrifugal CCC and both packed and open tubular LC, it is apparent that additional factors must be considered. The mass transfer terms as represented in eq 4–6 are operative in centrifugal CCC. These factors most likely are responsible for the observed decrease in efficiency as the flow rate increases from 0 to about 2.0 mL/min (Figures 3 and 4). However in centrifugal CCC, further increases in the flow rate significantly increase the efficiency of the separation process. It seems that traditional forms of the van Deemter and other related flow-efficiency equations cannot explain (either qualitatively or quantitatively), the data in this study. In addition, there are no reports that explain the relationship between the various experimental parameters and the observed back pressure in centrifugal CCC, to our knowledge.

THEORY

Model. A model can be formulated to account for the observed flow efficiency behavior. A single channel or cell in the CPC apparatus has a cross-sectional area (A_c) and a total volume (V_t). V_t is divided into the stationary phase volume (V_s) and the mobile phase volume (V_m). The extraction process is divided conceptually into three stages. Initially, the cell contains only the less dense stationary phase. The mobile phase is introduced at the top of the stationary phase as N_D droplets of volume V_D and surface area A_D. These drops fall through the stationary phase with velocity (υ), exchanging solute across a surface area (A_1) for a period of time (t_1). Normally, this time is very short, particularly at higher flow rates where streaming occurs. The drops or streams do not immediately coalesce with the pool of mobile phase at the end of the chamber. Rather, it exists for a period of time as droplets in an emulsified band between the two bulk phases (Figure 1). Solute exchange continues during this period, still across the surface area ($A_2 = N_D A_D$). The average time of residence in this settling condition (t_2), is assumed to be proportional to the flow rate raised to some power, since agitation by flow stirs the boundary and broadens the emulsified band. This time is expected to be inversely related to the velocity of the falling droplets, since those factors that increase the velocity (difference in density, centrifugal force, fluidity, etc.) tend to decrease the time of settling and the thickness of the band. Surface tension should also have an inverse effect on this time.

The remainder of the residence time (t_3) is spent in a fairly quiescent state with stirred but nonturbulent exchange across the cross-sectional area ($A_3 = A_c$). The total residence time ($t = t_1 + t_2 + t_3$) is equal to the volume of the mobile phase divided by the flow rate ($t = V_m/F$). After this time, the mobile phase is removed and the process is repeated in the next cell.

Kinetic Considerations. Long residence times and high surface areas facilitate the attainment of equilibrium and maximum efficiency of the exchange process. The time of falling is independent of flow rate per se, and this stage of the process is not expected to be of major importance. At very slow flow rates, residence times approach infinity allowing attainment of equilibrium across the relatively small cross-sectional area (A_c). Increasing the flow rate decreases the total time of residence, and thus decreases the efficiency of the exchange if kinetic factors are important. However, as the flow rate increases, there is an increase in the amount of

emulsified region as well as a decrease in the size of the emulsified droplets. This results in an increased surface area, thereby increasing the efficiency of the process. Also, effective mixing of the two phases may be better at higher flow rates, which would improve efficiency. By analogy, one could obtain similar results in traditional packed or open tubular chromatography only if the diameter of the packing or tubing and the thickness of the stationary phase reversibly decreased with increasing flow rate. This, of course, is unlikely. Unfortunately, one cannot increase the flow rate of centrifugal CCC indefinitely because eventually the broadening emulsified region will approach the exit port and "flooding" will occur.

Kinetic Formulation Based on Centrifugal CCC Model. In the aforementioned CCC model, the maximum efficiency that can be achieved is one plate per channel. If a channel was sufficiently long and a concentration gradient developed along its length and the exchange process was relatively rapid compared to the rate of mobile phase droplet descent time (t_1), then it might be possible to obtain more than one plate per channel. However, this has not been observed, as yet, for any solute in any liquid–liquid system, even though a variety of operation conditions were employed. If the efficiency is poor, the solute may flow through several channels before achieving one theoretical plate. Hence, in this treatment efficiency (E) will be defined as the ratio of the change in concentration of solute actually occurring in the mobile phase over the change that would occur in the mobile phase if the system were allowed to reach equilibrium

$$E = (C_m - C_{m,0})/(C_{m,eq} - C_{m,0}) = (C_s - C_{s,0})/(C_{s,eq} - C_{s,0}) \quad (7)$$

where C_m is the concentration of solute actually in the mobile phase of a given chamber, $C_{m,0}$ is the concentration of solute in the mobile phase before any equilibration has taken place, and $C_{m,eq}$ is the concentration of solute in the mobile phase if the system were isolated and allowed to reach equilibrium. If optimum efficiency is achieved, then $C_m = C_{m,eq}$ and $E = 1$. This occurs at zero flow rate and occasionally at high flow rates (see Figure 3). In all other cases, $C_m \neq C_{m,eq}$ and $E < 1$. E also corresponds to the fraction of plates per channel. Also

$$(1 - E) = (C_{m,eq} - C_m)/C_{m,eq} - C_{m,0}) \quad (8)$$

In this CPC model, the exchange of solute between stationary and mobile phase liquids occurs in three stages. The first stage exchange is between the falling droplets or stream and the surrounding stationary liquid. The second stage is the exchange in the emulsified region where the settling and separation of phases occur. The third exchange stage is between the quiescent pool of mobile phase at one end of the channel and the stationary phase. All exchange processes are assumed to be first order. In this case

$$dM_m/dt = (A_D)(k_{sm}C_s - k_{ms}C_m) \quad (9)$$

and

$$dC_m/dt = (A_{(t)}/V_m)(k_{sm}C_s - k_{ms}C_m) \quad (10)$$

where M_m is the moles of solute in the mobile phase droplet, t is time, $A_{(t)}$ is the surface area at time, t, C_s is the concentration of solute in the stationary phase, C_m is the concentration of solute in the mobile phase, k_{sm} is the rate of transfer of solute from stationary to mobile phase, k_{ms} is the rate of transfer of solute from mobile to stationary phase, and V_m is the volume of mobile phase. A partition coefficient (P') is defined as

$$P' = k_{sm}/k_{ms} = C_{m,eq}/C_{s,eq} \quad (11)$$

This is the reciprocal of the standard partition coefficient. From the conservation of mass one obtains

$$C_sV_s + C_mV_m = C_{s,eq}V_s + C_{m,eq}V_m \quad (12)$$

where V_s is the volume of stationary phase. Solving eq 12 for C_s and substituting P' where appropriate

$$C_s = C_{m,eq}(1/P' + V_m/V_s) - C_mV_m/V_s \quad (13)$$

Substituting for k_{ms} and C_s in eq 10 and rearranging

$$dC_m/dt = (A_{(t)}/V_m)k_{sm}(1/P' + V_m/V_s)(C_{m,eq} - C_m) \quad (14)$$

Integrating eq 14 between t_i and t_j

$$-\ln [(C_{m,eq} - C_{m,i})/C_{m,eq} - C_{m,j})] = (A_{(t)}/V_m)k_{sm}(1/P' + V_m/V_s)(t_i - t_j) \quad (15)$$

Let $P = P'V_m/V_s = M_{m,eq}/M_{s,eq}$

$$-\ln [(C_{m,eq} - C_{m,i})/(C_{m,eq} - C_{m,j})] = (A_{(t)}/PV_s)k_{sm}(1 + P)(t_i - t_j) \quad (16)$$

For the three stages of the process

$$-\ln [(C_{m,eq} - C_{m,1})/(C_{m,eq} - C_{m,0})] = (t_1A_1/PV_s)k_{sm}(1 + P) \quad (17)$$

$$-\ln [(C_{m,eq} - C_{m,2})/(C_{m,eq} - C_{m,1})] = (t_2A_2/PV_s)k_{sm}(1 + P) \quad (18)$$

$$-\ln [(C_{m,eq} - C_{m,3})/(C_{m,eq} - C_{m,2})] = (t_3A_3/PV_s)k_{sm}(1 + P) \quad (19)$$

Summing the three stages

$$-\ln [(C_{m,eq} - C_{m,3})/(C_{m,eq} - C_{m,0})] = (k_{sm}/PV_s)(1 + P)(t_1A_1 + t_2A_2 + t_3A_3) \quad (20)$$

Given our definition of efficiency (eq 7 and 8) it is apparent that

$$-\ln (1 - E) = (k_{sm}/PV_s)(1 + P)(t_1A_1 + t_2A_2 + t_3A_3) \quad (21)$$

Since $t = t_1 + t_2 + t_3$

$$-\ln (1 - E) = (k_{sm}/PV_s)(1 + P)[tA_c + t_1(A_1 - A_c) + t_2(A_2 - A_c)] \quad (22)$$

where A_c is the cross-sectional area of a channel, which is the same as the surface area of the quiescent phase. If the falling stage is very quick, then

$$-\ln (1 - E) = (k_{sm}/PV_s)(1 + P)[tA_c + t_2(N_DA_D - A_c)] \quad (23)$$

where N_D is the number of droplets and A_D is the surface area of the droplet.

Since the overall time is inversely proportional to flow rate, F ($t = V_m/F$), and the settling time ($t_2 = B'F^b$) is proportional to the flow rate raised to some power (b), eq 23 can be written

$$-\ln (1 - E) = A/F + BF^b \quad (24)$$

where $A = QV_mA_c$, $B = QB'(N_DA_D - A_c)$, $Q = (k_{sm}/PV_s)(1 + P)$, and $B/A = (B'/V_mA_c)(N_DA_D - A_c)$. The absolute values of the parameters A and B will depend on the solute (k_{sm},P) as well as the solvent system and the conditions of the experiment, but the value of b and the ratio B/A should be independent of the solute, provided it has no surfactant effect on the system.

The fraction of the total time that is spent in the emulsified region (f_e) is given by

$$f_e = t_2/t = B'F^{1+b}/V_m \quad (25)$$

and

$$f_e = (BA_c/A)F^{1+b}/(N_DA_D - A_c) \quad (26)$$

but

$$N_D = V_m/V_D = h_mA_c/V_D \quad (27)$$

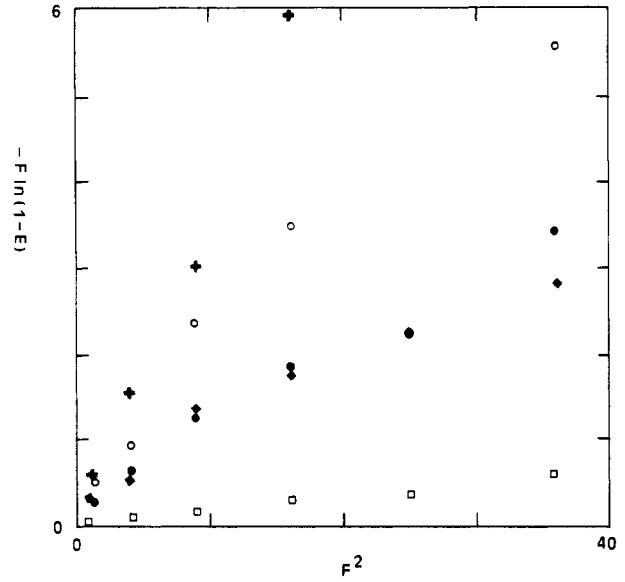

Figure 5. Plot of efficiency $[-F \ln (1 - E)]$ versus F^{b+1} for $b = 1$. This shows the correlation of the derived theory (eq 24), with the experimental results for DDT (●), DDD (◆), 1-naphthol (+), hydroquinone (□) and pentachlorophenol (○).

with h_m representing the height of the mobile phase (at very low flow rates, i.e., no emulsified layer) in the cell, and

$$N_D A_D / A_c = 3h_m / R_D \quad (28)$$

and

$$f_e = (B/A)F^{1+b}/(3h_m/R_D - 1) \quad (29)$$

with R_D representing the average radius of a droplet in the emulsified region.

When the time spent in the emulsified region approaches the total time of extraction ($f_e \rightarrow 1$), the mobile phase is becoming totally emulsified, and "flooding" will occur. The flow rate at the onset of "flooding" (F_f) is given by

$$F_f^{1+b} = V_m/B' = (A/B)(3h_m/R_D - 1) \quad (30)$$

$$f_e = (F/F_f)^{1+b} \quad (31)$$

The parameter B' relates the time spent in the emulsified layer to the flow rate, and is inversely related to the settling rate. The settling rate is expected to be proportional to the square of the angular velocity (ω), and eq 30 leads to

$$F_f^{1+b} = \text{constant} \times V_m \omega^2 \quad (32)$$

with the constant dependent on properties of the system (viscosity and density of the phases, surface tension, etc.) and on the conditions of the experiment (temperature, size of rotor, ascending or descending mode). The flooding flow rate, volume of the mobile phase, and the angular velocity are seen to be very closely related.

This relationship is determined by the start-up conditions for the experiment. The apparatus is first filled with the stationary phase. The device is then rotated at some angular velocity (ω^*) while the mobile phase is pumped through at the flow rate (F^*). Eventually a steady state is reached, which establishes the mobile phase volume (V_m). F^* approaches the flooding rate for the conditions of V_m and ω^*

$$F^{*1+b} = \text{constant} \times V_m \omega^{*2} \quad (33)$$

The experiment is then performed at either a higher angular velocity or a lower flow rate, fixing the mobile phase volume at V_m, except for "bleeding" effects (*13*). Combination of eq 32 and 33 then gives the flooding flow rate for these new conditions in terms of the start-up conditions

$$F_f/F^* = (\omega/\omega^*)^{2/(1+b)} \quad (34)$$

Table I. Calculation of Parameters from Efficiency Equation (Equation 24)[a]

solute	b	A, cm³/min	$B^{1/b}$, min/cm³	A/B
		System: Hexane + Methanol (water)		
β-naphthol	1.0	0.25 ± 0.03	0.32 ± 0.03	0.76 ± 0.08
	0.5	0.20 ± 0.06	0.29 ± 0.10	0.36 ± 0.12
DDD	1.0	0.14 ± 0.03	0.18 ± 0.02	0.77 ± 0.10
	0.5	0.10 ± 0.02	0.14 ± 0.02	0.26 + 0.04
DDT	1.0	0.07 ± 0.01	0.11 ± 0.01	0.66 ± 0.14
	0.5	0.046 ± 0.005	0.05 ± 0.01	0.20 ± 0.02
		System: Octanol + Water		
pentachloro-	1.0	0.18 ± 0.01	0.07 ● 0.005	2.5 ± 0.2
phenol	0.5	0.16 ± 0.01	0.029 ± 0.002	0.93 ± 0.07
hydroquinone	1.0	0.035 ± 0.003	0.014 ± 0.001	2.6 ± 0.3
	0.5	0.031 ± 0.002	0.0010 ± 0.0001	1.0 ± 0.1

[a] All calculations were done by using eq 24 in the following form: $-F \ln (1 - E) = A + BF^{b+1}$. the regression was weighted to minimize deviations in $\ln (1 - E)$ rather than in $F \ln (1 - E)$. This gives greater reliability in values of A, but slightly lower correlation coefficients.

Table II. Values of Flooding Flow Rates (F_f) Calculated from Equation 30[a]

solute	b	F_f
	Hexane (Methanol/Water) System	
β-Naphthol	1.0	5.2 ± 0.3
	0.5	5.4 ± 1.2
DDD	1.0	5.2 ± 0.3
	0.5	4.4 ± 0.4
DDT	1.0	4.8 ± 0.5
	0.5	3.7 ± 0.3
	Octanol–Water System	
pentachlorophenol	1.0	9.4 ± 0.4
	0.5	10.2 ± 0.5
hydroquinone	1.0	9.5 ± 0.6
	0.5	10.7 ± 0.7

[a] Based on $h_m = 0.6$ cm and $R_D = 0.05$ cm.

The relevant parameters for the derived efficiency equation (eq 24) can be calculated from experimental data (Figures 3 and 4) by using a linear regression of $-F \ln (1 - E)$ versus F^{b+1}. This relationship with $b = 1$ is shown graphically in Figure 5. In most cases, there was better linearity with $b = 1$, but in some cases $b = {}^1/_2$ gave the better fit. The values of A and B reported in Table I were calculated with a weighted least-squares regression, which minimizes the sum of squares of the deviations in the quantity $\ln (1 - E)$. This procedure gives substantially lower uncertainties in the intercept (A) and slightly higher uncertainties in the slope (B) than the unweighted procedure, which minimizes the sum of squares of deviations in $F \ln (1 - E)$. Note the relative constancy of the ratio A/B for a given value of b for each of the solvent systems studied.

Values were calculated for the flooding flow rate from (eq 30) by using the radius of the connecting duct as the radius of the droplet, and these results are given in Table II. These results are in qualitative agreement with observed values, which were of the order of 7–9 mL/min, with higher values for the more viscous octanol–water system.

Table III lists the calculated mass transfer coefficients. The partition coefficients of β-naphthol, DDD, DDT, and hydroquinone were determined experimentally while that of pentachlorophenol was taken from the literature (*21*).

In all, the descriptive and mathematical models fit the experimentally observed nonequilibrium behavior of centrifugal CCC. It is also apparent that the geometry of the flow chambers plays an important role in efficiency, flooding flow rate, and so on. This parameter is being investigated currently.

Table III. Calculated Values of the Mass Transfer Coefficients[a]

solute:	P^*	b	A, cm³/min	k_{sm}, cm/min	k_{ms}, cm/min
β-naphthol	0.17	1	0.25 ± 0.03	4.8 ± 0.6	0.8 ± 0.1
		0.5	0.20 ± 0.06	3.8 ± 1.1	0.6 ± 0.2
DDD	0.47	1	0.14 ± 0.03	2.3 ± 0.5	1.1 ± 0.2
		0.5	0.10 ± 0.02	1.6 ± 0.3	0.8 ± 0.1
DDT	0.96	1	0.07 ± 0.01	0.91 ± 0.10	0.88 ± 0.10
		0.5	0.046 ± 0.005	0.60 ± 0.06	0.58 ± 0.06
pentachloro-phenol	10^{-5}	1	0.18 ± 0.01	3.8 ± 0.2	3.8×10^{-5}
		0.5	0.16 ± 0.01	3.4 ± 0.2	3.4×10^{-5}
hydro-quinone	0.34	1	0.035 ± 0.003	0.60 ± 0.05	0.21 ± 0.02
		0.5	0.031 ± 0.002	0.54 ± 0.03	0.18 ± 0.01

[a] The kinetic coefficients, k_{sm} and k_{ms}, can be determined from the parameter A: $A = QV_mA_c$, $Q = (k_{sm}/PV_s)(1 + P)$. P' has been defined as the reciprocal of the normal partition coefficient, so the normal partition coefficient is defined here as P^* where $P = V_m/V_sP^*$, $A = k_{sm}A_c(V_sP^* + V_m)/V_s$, $k_{sm} = AV_s/A_c(V_sP^* + V_m)$, and $k_{ms} = k_{sm}P^*$. The value of A to be used in this calculation is relatively independent of the form of the equation (value of b) chosen. Calculations are based on V_m = 75 cm³, V_s = 50 cm³, and A_c = 0.031 cm².

Factors Affecting Back Pressure. In most centrifugal CCC experiments there is a significant pressure drop. A variety of experimental variables seem to affect the pressure, but these have not been elucidated in any detail. The unit itself has a pressure limit of 850 psi. Many of the things that control efficiency in centrifugal CCC (e.g., flow rate, rotation rate, solvent viscosity, etc.) also affect the system back pressure. Consequently, one must consider all of these things when carrying out a separation. The factors that contribute to back pressure can be divided into hydrostatic and hydrodynamic terms.

The hydrostatic equation that relates the change in pressure, ΔP, between the top and bottom of a channel filled with liquid in a gravitational field is

$$\Delta P = \rho\sigma h_c \tag{35}$$

where ρ is the density of the liquid (kg/m³), h_c is the channel height, and σ is the gravitational force constant. In CPC a centrifuge is used, therefore the gravitational constant must be replaced by ω^2R_r to give

$$\Delta P = \rho\omega^2R_rh_c \tag{36}$$

where ω is the angular velocity (radians per second) and R_r is the radius of the rotor. In CPC the channels contain two immiscible liquids (the stationary phase and the mobile phase, see Figure 1). When the second liquid is present in the system the pressure drop in the connecting duct (which contains only the mobile phase) does not compensate exactly the pressure drop in the channel (which contains both liquids). The residual pressure depends on the density difference between the two liquids, $\Delta\rho$, and the height of the stationary phase in one channel, h_s. Therefore the hydrostatic term for CPC is

$$\Delta P = n\,\Delta\rho\,\omega^2R_rh_s \tag{37}$$

where n is the total number of channels in the system.

Hydrodynamics also contributes to the observed back pressure in centrifugal CCC. This term can be derived from Poiseuille's law for an open tube

$$\Delta P = 8\eta LF/(\pi r^4) \tag{38}$$

where ΔP is the pressure difference (N/m²), η is the liquid mobile phase viscosity (kg/m s), L is the tube length (m), r is the tube radius (m), and F is the flow rate (m³/s). The ratio $8L/\pi r4$ will be referred to as the coefficient γ (m⁻³) and is related to the geometric characteristics of the tube. The complete equation relating pressure to hydrostatic and hydrodynamic terms is

$$P = n[\Delta\rho\,\omega^2R_rh + \eta\gamma F] \tag{39}$$

While the shape of the channels (Figure 1) cannot be considered an open tube of constant radius, the γ value of eq 39 is the same as an open tube of flow characteristics equivalent to a channel plus its duct. Indeed, the γ value can be estimated by

$$\gamma = [\Delta P \text{ per channel} - \Delta\rho\,\omega^2R_rh_s]/\eta F \tag{40}$$

The relative importance of the hydrostatic and hydrodynamic contributions depends on the chosen experimental conditions (*13*). For example, the hydrostatic term would be dominant if two liquids that have a large difference in densities but low viscosities are chosen (e.g., hexane and water). Conversely the hydrodynamic term becomes dominant if the viscosity of the mobile phase is high and the difference in density is low (e.g., octanol and water). The hydrodynamic term becomes more important at higher flow rates. The rotation rate remains one of the most important parameters acting on the pressure drop. This is because the pressure increases with the square of the angular velocity (see ω^2 in eq 39). Further experimental verification of eq 39 has been reported recently (*13*, *14*).

CONCLUSIONS

It is apparent from the flow efficiency profiles (Figures 3 and 4) that centrifugal countercurrent chromatography may be well suited for both preparative and high-velocity separations. This is because of the unusual tendency of this technique to become more efficient at higher flow rates. However, the flow rate cannot be raised indefinitely. There are two factors that limit this. One is flooding (i.e., the point at which the emulsified stationary and mobile phases are coeluted) and the other is the pressure limitations of the unit (i.e. mainly the rotary seal and the PCTFE cartridges plus connecting tubing). The mixing of the mobile phase with the stationary phase is controlled by not only the flow rate but also the geometry of the channels. A differently designed channel might allow the attainment of higher flow rates before flooding. Increasing the rotation rate of the centrifuge also inhibits flooding at a given flow rate (eq 32). However, small increases in the angular velocity substantially increase the back pressure (eq 39). Eventually this forces one to decrease the flow rate in order to keep from exceeding the pressure limits of the unit. This is indicative of the trade-offs that must be considered when preparing for separations of this kind.

In traditional HPLC the choice of stationary phase and mobile phase is dictated largely by selectivity considerations. Selectivity is also an important factor in choosing these phases for centrifugal CCC. However, the relative viscosities and densities of the stationary and mobile phase liquids must also be considered carefully. These factors can control or limit the separation efficiency (see Figure 3 vs Figure 4), the system pressure and flow rate (eq 39). In general, effective optmization of centrifugal CCC separations requires a more detailed knowledge of the physicochemical properties of a variety of solvent systems and the solutes being separated.

GLOSSARY

A	efficiency constant (cm³/min)
A_c	cross-sectional area of a single channel (cm²)
A_D	surface area of a mobile phase droplet (cm²)
A_1	interface area between the moving droplets and the stationary phase (cm²)
A_2	interface area between the droplets in the emulsified band and the stationary phase (cm²)
A_3	$=A_c$

$A_{(t)}$ interface area at time t (cm^2)
b flow rate exponent in the efficiency relation (dimensionless)
B efficiency parameter $(cm^3/min)^{-b}$
B' intermediate parameter $(=t_2/F^b)$
C_m actual concentration of the solute in the mobile phase (mol/cm^3)
$C_{m,eq}$ concentration of the solute in the mobile phase when the equilibrium with the stationary phase is reached (mol/cm^3)
$C_{m,0}$ concentration of the solute in the mobile phase before any equilibration (mol/cm^3)
C_s actual concentration of the solute in the stationary phase (mol/cm^3)
$C_{s,eq}$ see $C_{m,eq}$ (mol/cm^3)
$C_{s,0}$ see $C_{m,0}$ (mol/cm^3)
d_f thickness of the stationary phase layer accessible to the solute (cm)
d_p particle size diameter of a solid stationary phase (cm)
D_m solute diffusion coefficient in the mobile phase (cm^2/s)
D_s solute diffusion coefficient in the stationary phase (cm^2/s)
E efficiency defined as the fraction of a plate per actual channel ($E < 1$, a dimensionless parameter)
f_e fraction of time spent by a droplet in the emulsified band ($=t_2/t$, dimensionless)
F mobile phase flow rate (mL/min)
F_f "flooding" flow rate (mL/min)
h channel height (cm)
h_m height of the quiet mobile phase in a channel (cm)
h_s height of the stationary phase in a channel (cm)
H height equivalent to a theoretical plate (cm)
H_e plate height contribution due to eddy diffusion (cm)
H_m plate height contribution due to moving mobile phase effects (cm)
H_s plate height contribution due to stationary phase mass transfer (cm)
H_{sm} plate height contribution to stagnant stationary phase mass transfer (cm)
H_D plate height contribution due to gradient concentration diffusion (cm)
H_L plate height contribution for longitudinal diffusion (cm)
k' capacity factor of a solute (dimensionless)
k_{ms} rate constant of the transfer of solute from mobile phase to stationary phase (cm/s)
k_{sm} rate constant of the transfer of solute from stationary phase to mobile phase (cm/s)
M_m moles of solute in the mobile phase
M_s moles of solute in the stationary phase
n plate number
N_D number of droplets in the emulsified band (dimensionless)
P partition coefficient expressed as the mass ratio M_m/M_s (dimensionless)
P' partition coefficient expressed as the concentration ratio, $P' = PV_s/V_m$
q "configuration factor" (cm^{-1})
Q $=(1 + P)(k_{sm}/PV_s)$
R_D average radius of a droplet in the emulsified band (cm)
R_r rotor radius (cm)
t total residence time of a theoretical droplet of mobile phase in the stationary phase contained in one channel $= t_1 + t_2 + t_3$ (s)
t_1 mean falling time of a droplet through the stationary phase (s)
t_2 mean residence time of a droplet in the emulsified band (s)
t_3 mean theoretical residence time of a coalesced droplet in the mobile phase pool existing in each channel (s)
T_m Golay term related to mobile phase mass transfer (s)
T_s Golay term related to stationary phase mass transfer (s)
v velocity of a mobile phase droplet in the stationary phase (cm/s)
V_D mean volume of the droplet in the stationary phase (cm^3 or mL)
V_m mobile phase volume in a channel (mL)
V_s stationary phase volume in a channel (mL)
V_t total channel volume (mL)

GREEK SYMBOLS

β "tortuosity" parameter (cm^{-1})
η stationary phase viscosity (cP or g/(cm s) × 100)
γ coefficient related to the channel geometry (cm^{-3})
ν mobile phase flow velocity (cm/s)
ω spin rate (rad/s)
$\Delta\rho$ density difference between phases (g/mL)
ΔP pressure drop in the CPC rotor (9.81 kg/cm^2)

LITERATURE CITED

(1) Ito, Y.; Weinstein, M.; Aoki, I.; Harada, R.; Kimura, E.; Nunogaki, K. *Nature (London)* **1966**, *212*, 985.
(2) Ito, Y.; Bhatnagar, R. *J. Liq. Chromatogr.* **1984**, *7*, 257.
(3) Sutherland, A.; Heywood-Waddington, D.; Peters, T. J. *J. Liq. Chromatogr.* **1984**, *7*, 363.
(4) Flanagan, S. D.; Johansson, G.; Yost, B.; Ito, Y.; Sutherland, I. A. *J. Liq. Chromatogr.* **1984**, *7*, 385.
(5) Signer, R.; Allenmann, K.; Koehli, E.; Lehmann, W.; Mayer, H.; Ritschard, W. *DECHEMA Monogr.* **1956**, *27*, 36.
(6) Signer, R.; Arm, H. *Helv. Chim. Acta* **1967**, *50*, 46.
(7) Snyder, J. K.; Nakanishi, K.; Hostettman, K.; Hostettmann, M. *J. Liq. Chromatogr.* **1984**, *7*, 243.
(8) Tanimura, T.; Pisano, J. J.; Ito, Y.; Bowmann, R. L. *Science (Washington, D.C.)* **1970**, *169*, 54.
(9) Hostettmann, K.; Appolonia, B.; Domon, B.; Hostettmann, M. *J. Liq. Chromatogr.* **1984**, *7*, 231.
(10) Murayama, W.; Kobayashi, T.; Kosuge, Y.; Yano, H.; Nunogaki, Y.; Nunogaki, K. *J. Chromatogr.* **1982**, *239*, 643.
(11) *Centrifugal Partition Chromatograph Model NMF*; Technical Information; Sanki Laboratories: Sharon Hill, PA, 1987.
(12) *J. Liq. Chromatogr.* **1984**, *7*, 227–440.
(13) Berthod, A.; Armstrong, D. W. *J. Liq. Chromatogr.* **1988**, *11*, 547.
(14) Berthod, A.; Armstrong, D. W. *J. Liq. Chromatogr.* **1988**, *11*, 567.
(15) Van Deemter, J. J.; Zuiderweg, F. J.; Klinkenberg, A. *Chem. Eng. Sci.* **1956**, *5*, 271.
(16) Giddings, J. C. *Dynamics of Chromatography*; Dekker: New York, 1965; Part 1.
(17) Golay, M. J. E. *Gas Chromatography*; Amsterdam Symposium; Desty, D. H., Ed.; Butterworths: London, 1956; pp 36–55.
(18) Kaiser, R. *Gas Phase Chromatography Vol. II, Capillary Chromatography*; Butterworths: Washington, DC, 1963; pp 1–22.
(19) Szepesy, L. *Gas Chromatography*; CRC Press: Cleveland, OH, 1970; pp 53–91.
(20) Tyssen, R. *Anal. Chim. Acta* **1980**, *114*, 71.
(21) Leo, A.; Hansch, C.; Elkins, D. *Chem. Rev.* **1971**, *71*, 525.

RECEIVED for review March 24, 1988. Accepted August 18, 1988. Support of this work by the National Institute of General Medical Sciences (BMT 1R01 GM36292) is gratefully acknowledged.